

PHYSICAL REVIEW D

PARTICLES AND FIELDS

THIRD SERIES, VOLUME 49, NUMBER 1

1 JANUARY 1994

RAPID COMMUNICATIONS

Rapid Communications are intended for important new results which deserve accelerated publication, and are therefore given priority in editorial processing and production. A Rapid Communication in Physical Review D should be no longer than five printed pages and must be accompanied by an abstract. Page proofs are sent to authors, but because of the accelerated schedule, publication is generally not delayed for receipt of corrections unless requested by the author.

Measurement of Drell-Yan electron and muon pair differential cross sections in $\bar{p}p$ collisions at $\sqrt{s} = 1.8$ TeV

F. Abe,¹² M. Albrow,⁶ D. Amidei,¹⁵ C. Anway-Wiese,³ G. Apollinari,²³ M. Atac,⁶
 P. Auchincloss,²² P. Azzi,¹⁷ N. Bacchetta,¹⁶ A. R. Baden,⁸ W. Badgett,¹⁵ M. W. Bailey,²¹ A. Bamberger,⁶
 P. de Barbaro,²² A. Barbaro-Galtieri,¹³ V. E. Barnes,²¹ B. A. Barnett,¹¹ G. Bauer,¹⁴ T. Baumann,⁸ F. Bedeschi,²⁰
 S. Behrends,² S. Belforte,²⁰ G. Bellettini,²⁰ J. Bellinger,²⁸ D. Benjamin,²⁷ J. Benlloch,¹⁴ J. Bensinger,²
 A. Beretvas,⁶ J. P. Berge,⁶ S. Bertolucci,⁷ K. Biery,¹⁰ S. Bhadra,⁹ M. Binkley,⁶ D. Bisello,¹⁷
 R. Blair,¹ C. Blocker,² K. Bloom,⁴ A. Bodek,²² V. Bolognesi,²⁰ A. W. Booth,⁶ C. Boswell,¹¹
 G. Brandenburg,⁸ D. Brown,⁸ E. Buckley-Geer,⁶ H. S. Budd,²² G. Busetto,¹⁷ A. Byon-Wagner,⁶ K. L. Byrum,¹
 C. Campagnari,⁶ M. Campbell,¹⁵ A. Caner,⁶ R. Carey,⁸ W. Carithers,¹³ D. Carlsmith,²⁸ J. T. Carroll,⁶
 R. Cashmore,⁶ A. Castro,¹⁷ Y. Cen,¹⁸ F. Cervelli,²⁰ K. Chadwick,⁶ J. Chapman,¹⁵ G. Chiarelli,⁷
 W. Chinowsky,¹³ S. Cihangir,⁶ A. G. Clark,⁶ M. Cobal,²⁰ D. Connor,¹⁸ M. Contreras,⁴ J. Cooper,⁶
 M. Cordelli,⁷ D. Crane,⁶ J. D. Cunningham,² C. Day,⁶ F. DeJongh,⁶ S. Dell'Agnello,²⁰ M. Dell'Orso,²⁰
 L. Demortier,²³ B. Denby,⁶ P. F. Derwent,¹⁵ T. Devlin,²⁴ D. DiBitonto,²⁵ M. Dickson,²² R. B. Drucker,¹³
 A. Dunn,¹⁵ K. Einsweiler,¹³ J. E. Elias,⁶ R. Ely,¹³ S. Eno,⁴ S. Errede,⁹ A. Etchegoyen,⁶
 B. Farhat,¹⁴ M. Frautschi,¹⁶ G. J. Feldman,⁸ B. Flaughner,⁶ G. W. Foster,⁶ M. Franklin,⁸ J. Freeman,⁶
 H. Frisch,⁴ T. Fuess,⁶ Y. Fukui,¹² A. F. Garfinkel,²¹ A. Gauthier,⁹ S. Geer,⁶ D. W. Gerdes,¹⁵
 P. Giannetti,²⁰ N. Giokaris,²³ P. Giromini,⁷ L. Gladney,¹⁸ M. Gold,¹⁶ J. Gonzalez,¹⁸ K. Goulios,²³
 H. Grassmann,¹⁷ G. M. Grieco,²⁰ R. Grindley,¹⁰ C. Grosso-Pilcher,⁴ C. Haber,¹³ S. R. Hahn,⁶ R. Handler,²⁸
 K. Hara,²⁶ B. Harral,¹⁸ R. M. Harris,⁶ S. A. Hauger,⁵ J. Hauser,³ C. Hawk,²⁴ T. Hessing,²⁵
 R. Hollebeek,¹⁸ L. Holloway,⁹ A. Hölscher,¹⁰ S. Hong,¹⁵ G. Houk,¹⁸ P. Hu,¹⁹ B. Hubbard,¹³
 B. T. Huffman,¹⁹ R. Hughes,²² P. Hurst,⁸ J. Huth,⁶ J. Hysten,⁶ M. Incagli,²⁰ T. Ino,²⁶
 H. Iso,²⁶ H. Jensen,⁶ C. P. Jessop,⁸ R. P. Johnson,⁶ U. Joshi,⁶ R. W. Kadel,¹³ T. Kamon,²⁵
 S. Kanda,²⁶ D. A. Kardelis,⁹ I. Karliner,⁹ E. Kearns,⁸ L. Keeble,²⁵ R. Kephart,⁶ P. Kesten,²
 R. M. Keup,⁹ H. Keutelian,⁶ D. Kim,⁶ S. B. Kim,¹⁵ S. H. Kim,²⁶ Y. K. Kim,¹³ L. Kirsch,²
 K. Kondo,²⁶ J. Konigsberg,⁸ K. Kordas,¹⁰ E. Kovacs,⁶ M. Krasberg,¹⁵ S. E. Kuhlmann,¹ E. Kuns,²⁴
 A. T. Laasanen,²¹ S. Lammel,³ J. I. Lamoureux,²⁸ S. Leone,²⁰ J. D. Lewis,⁶ W. Li,¹ P. Limon,⁶
 M. Lindgren,³ T. M. Liss,⁹ N. Lockyer,¹⁸ M. Loreti,¹⁷ E. H. Low,¹⁸ D. Lucchesi,²⁰ C. B. Luchini,⁹
 P. Lukens,⁶ P. Maas,²⁸ K. Maeshima,⁶ M. Mangano,²⁰ J. P. Marriner,⁶ M. Mariotti,²⁰ R. Markeloff,²⁸
 L. A. Markosky,²⁸ J. A. J. Matthews,¹⁶ R. Mattingly,² P. McIntyre,²⁵ A. Menzione,²⁰ E. Meschi,²⁰ T. Meyer,²⁵
 S. Mikamo,¹² M. Miller,⁴ T. Mimashi,²⁶ S. Miscetti,⁷ M. Mishina,¹² S. Miyashita,²⁶ Y. Morita,²⁶
 S. Moulding,²³ J. Mueller,²⁴ A. Mukherjee,⁶ T. Muller,³ L. F. Nakae,² I. Nakano,²⁶ C. Nelson,⁶
 D. Neuberger,³ C. Newman-Holmes,⁶ J. S. T. Ng,⁸ M. Ninomiya,²⁶ L. Nodulman,¹ S. Ogawa,²⁶ R. Paoletti,²⁰
 V. Papadimitriou,⁶ A. Para,⁶ E. Pare,⁸ S. Park,⁶ J. Patrick,⁶ G. Pauletta,²⁰ L. Pescara,¹⁷
 T. J. Phillips,⁵ A. G. Piacentino,²⁰ R. Plunkett,⁶ L. Pondrom,²⁸ J. Proudfoot,¹ F. Ptohos,⁸ G. Punzi,²⁰
 D. Quarrie,⁶ K. Ragan,¹⁰ G. Redlinger,⁴ J. Rhoades,²⁸ M. Roach,²⁷ F. Rimondi,^(6,a) L. Ristori,²⁰
 W. J. Robertson,⁵ T. Rodrigo,⁶ T. Rohaly,¹⁸ A. Roodman,⁴ W. K. Sakumoto,²² A. Sansoni,⁷ R. D. Sard,⁹
 A. Savoy-Navarro,⁶ V. Scarpine,⁹ P. Schlabach,⁸ E. E. Schmidt,⁶ O. Schneider,¹³ M. H. Schub,²¹ R. Schwitters,⁸
 G. Sciacca,²⁰ A. Scribano,²⁰ S. Segler,⁶ S. Seidel,¹⁶ Y. Seiya,²⁶ G. Sganos,¹⁰ M. Shapiro,¹³
 N. M. Shaw,²¹ M. Sheaff,²⁸ M. Shochet,⁴ J. Siegrist,¹³ A. Sill,²² P. Sinervo,¹⁰ J. Skarha,¹¹
 K. Sliwa,²⁷ D. A. Smith,²⁰ F. D. Snider,¹¹ L. Song,⁶ T. Song,¹⁵ M. Spahn,¹³ P. Sphicas,¹⁴

A. Spies,¹¹ R. St. Denis,⁸ L. Stanco,¹⁷ A. Stefanini,²⁰ G. Sullivan,⁴ K. Sumorok,¹⁴ R. L. Swartz, Jr.,⁹ M. Takano,²⁶ K. Takikawa,²⁶ S. Tarem,² F. Tartarelli,²⁰ S. Tether,¹⁴ D. Theriot,⁶ M. Timko,²⁷ P. Tipton,²² S. Tkaczyk,⁶ A. Tollestrup,⁶ J. Tonnison,²¹ W. Trischuk,⁸ Y. Tsay,⁴ J. Tseng,¹¹ N. Turini,²⁰ F. Ukegawa,²⁶ D. Underwood,¹ S. Vejcek III,¹⁵ R. Vidal,⁶ R. G. Wagner,¹ R. L. Wagner,⁶ N. Wainer,⁶ R. C. Walker,²² J. Walsh,¹⁸ A. Warburton,¹⁰ G. Watts,²² T. Watts,²⁴ R. Webb,²⁵ C. Wendt,²⁸ H. Wenzel,²⁰ W. C. Wester III,¹³ T. Westhusing,⁹ S. N. White,²³ A. B. Wicklund,¹ E. Wicklund,¹ H. H. Williams,¹⁸ B. L. Winer,²² J. Wolinski,²⁵ D. Y. Wu,¹⁵ X. Wu,²⁰ J. Wyss,¹⁷ A. Yagil,⁶ K. Yasuoka,²⁶ Y. Ye,¹⁰ G. P. Yeh,⁶ J. Yoh,⁶ M. Yokoyama,²⁶ J. C. Yun,⁶ A. Zanetti,²⁰ F. Zetti,²⁰ S. Zhang,¹⁵ W. Zhang,¹⁸ and S. Zucchelli⁶

(CDF Collaboration)

¹Argonne National Laboratory, Argonne, Illinois 60439

²Brandeis University, Waltham, Massachusetts 02254

³University of California at Los Angeles, Los Angeles, California 90024

⁴University of Chicago, Chicago, Illinois 60637

⁵Duke University, Durham, North Carolina 27706

⁶Fermi National Accelerator Laboratory, Batavia, Illinois 60510

⁷Laboratori Nazionali di Frascati, Istituto Nazionale di Fisica Nucleare, Frascati, Italy

⁸Harvard University, Cambridge, Massachusetts 02138

⁹University of Illinois, Urbana, Illinois 61801

¹⁰Institute of Particle Physics, McGill University, Montreal, and University of Toronto, Toronto, Canada

¹¹The Johns Hopkins University, Baltimore, Maryland 21218

¹²National Laboratory for High Energy Physics (KEK), Japan

¹³Lawrence Berkeley Laboratory, Berkeley, California 94720

¹⁴Massachusetts Institute of Technology, Cambridge, Massachusetts 02139

¹⁵University of Michigan, Ann Arbor, Michigan 48109

¹⁶University of New Mexico, Albuquerque, New Mexico 87131

¹⁷Universita di Padova, Istituto Nazionale di Fisica Nucleare, Sezione di Padova, I-35131 Padova, Italy

¹⁸University of Pennsylvania, Philadelphia, Pennsylvania 19104

¹⁹University of Pittsburgh, Pittsburgh, Pennsylvania 15260

²⁰Istituto Nazionale di Fisica Nucleare, University and Scuola Normale Superiore of Pisa, I-56100 Pisa, Italy

²¹Purdue University, West Lafayette, Indiana 47907

²²University of Rochester, Rochester, New York 15627

²³Rockefeller University, New York, New York 10021

²⁴Rutgers University, Piscataway, New Jersey 08854

²⁵Texas A&M University, College Station, Texas 77843

²⁶University of Tsukuba, Tsukuba, Ibaraki 305, Japan

²⁷Tufts University, Medford, Massachusetts 02155

²⁸University of Wisconsin, Madison, Wisconsin 53706

(Received 1 June 1993)

We measure the Drell-Yan differential cross section $d^2\sigma/dM dy|_{|y|<1}$ over the mass range $11 < M < 150$ GeV/ c^2 using dielectron and dimuon data from $\bar{p}p$ collisions at a center-of-mass energy of $\sqrt{s} = 1.8$ TeV. Our results show the $1/M^3$ dependence that is expected from the naive Drell-Yan model. In comparison to the predictions of recent QCD calculations we find our data favor those parton distribution functions with the largest quark contributions in the x interval 0.006 to 0.03.

PACS number(s): 13.85.Qk, 12.38.Qk

The Drell-Yan process $q\bar{q} \rightarrow (\gamma, Z^0) \rightarrow l^+l^-$ is a probe of the parton distribution functions of the proton [1]. We present measurements of the differential cross section for electron and muon pair production, $d^2\sigma/dM dy|_{|y|<1}$, in $\bar{p}p$ collisions at a center-of-mass energy of $\sqrt{s} = 1.8$ TeV. The cross section is integrated over the rapidity interval $-1.0 < y < +1.0$, where y [2] is the rapidity of the lepton pair, and then divided by 2.0 to account for the two units of rapidity.

The data were collected with the Collider Detector at

Fermilab (CDF) during the 1988–1989 run. The sample used consists of dielectron and dimuon events of integrated luminosity \mathcal{L} of 4.13 pb⁻¹ and 2.77 pb⁻¹, respectively. The CDF is a large solenoidal magnetic spectrometer surrounded by calorimeters and muon detectors. The detector is described in detail in Ref. [3]. The fine-grain calorimeter segmentation and high-resolution central tracking allowed for excellent electron and muon identification as described in Refs. [4,5], respectively.

The range of dilepton invariant masses measured in

this experiment allows access to the small x region of the parton distribution functions down to $x=0.006$ [6,7], where x is defined as the fraction of proton momentum carried by the parton. This work complements our previous measurement of the Z° cross section [4,5] and our searches for new vector bosons and compositeness [8] in the dielectron and dimuon decay channels.

The on line trigger required all dilepton events to have at least one hit in each of the forward and backward scintillator arrays [9]. Dielectron events were selected by additionally requiring a trigger of two clusters of electromagnetic energy in the central calorimeter [10]. Each of the triggering clusters was required to have transverse electromagnetic energy [11] (E_T) > 5 GeV, a track associated with the cluster with transverse momentum (P_T) > 4.8 GeV/ c , and a ratio of hadronic to electromagnetic $E_T < 0.125$. The efficiency of this trigger, for a single electron, was determined as a function of E_T by studying events collected with an independent trigger. After reconstructing the events we required two clusters of electromagnetic $E_T > 5$ GeV in the central detector ($|\eta| < 1$) [12]. To maintain high detection efficiency, one electron candidate was required to satisfy a set of tight cuts and the other to pass a set of looser cuts. The tight cuts were identical to those of Ref. [13] with the exception of the cut value on the ratio of the calorimeter energy to track momentum, E/P , which was set to 1.5 instead of 2.0. The loose cuts differed from the tight ones in that the requirements were removed on energy sharing between adjacent towers and on lateral shower profile. The efficiency of these requirements, ϵ_{id} , was constant at 0.79 ± 0.03 for a wide range of electron E_T , as determined from Z° and J/ψ events. After these cuts 1111 dielectron events remained in the mass range $11 \leq M_{ee} \leq 150$ GeV/ c^2 .

Dimuon events were selected on line with a trigger that required two tracks in the central tracking chamber with $p_T > 3$ GeV/ c and matching tracks in the central muon chambers ($|\eta| < 0.6$) located outside the steel of the central hadron calorimeters [14]. The efficiency of this trigger, for a single muon, was determined as a function of p_T by studying muons from events collected with an independent trigger and from cosmic-ray events. After reconstruction we required one muon to have $p_T > 5$ GeV/ c and the other muon to have $p_T > 3$ GeV/ c . Both muon tracks had to match a track segment in the central muon chambers to within 10 cm in the $r-\phi$ plane [15]. Each muon was also required to deposit less than 2.0 GeV of energy in the electromagnetic calorimeter tower and less than 6.0 GeV of energy in the hadronic calorimeter tower which it traversed. The efficiency of these requirements, ϵ_{id} , was determined from Z° and J/ψ events to be 0.84 ± 0.05 . To reject cosmic-ray background events the opening angle between the two muons was required to be less than 175° and the impact parameters of both tracks with respect to the beam axis to be less than 0.15 cm. We were left with 832 dimuon events in the mass range $11 \leq M_{\mu\mu} \leq 150$ GeV/ c^2 .

Two sources dominate the background to the Drell-Yan signal: misidentification background and heavy quark decays. Misidentification background consists of

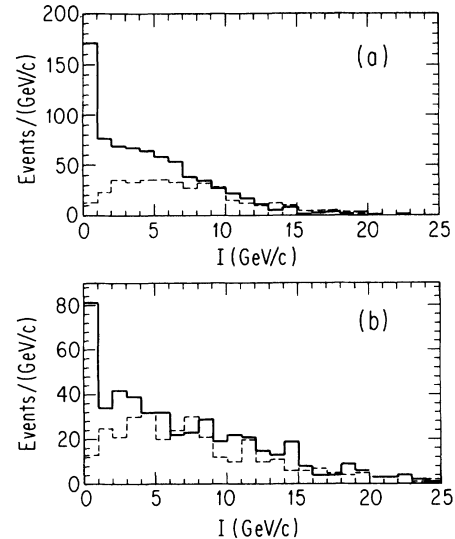


FIG. 1. The distribution of the isolation variable I for opposite-charged (solid line) and same-charged (dashed line) electron pairs (a) and muon pairs (b).

events with either an electron from a photon conversion, a lepton from the decay in flight of a hadron, or a misidentified hadron. The heavy quark decay background consists of pairs, mostly $b\bar{b}$, for which both quarks decay semileptonically. Both of these backgrounds originate predominantly from QCD jet events and tend to have nonisolated lepton candidates since the leptons are typically surrounded by other particles from the jet. Leptons from the Drell-Yan process have opposite charge, and are expected to be isolated. We defined an isolation variable, $I = \max(I_1, I_2)$, where the I_i are the

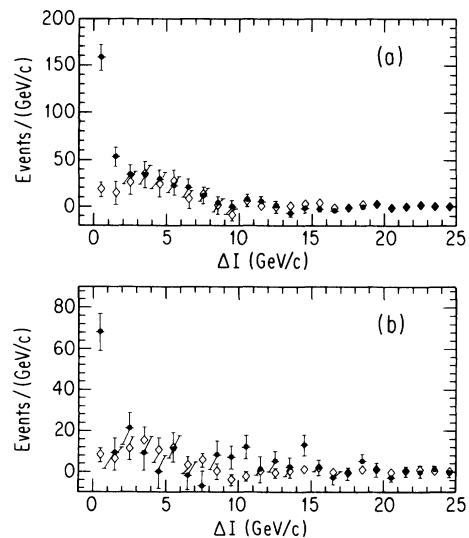


FIG. 2. Subtracted isolation distributions ΔI which result from subtracting the I distribution for same-charged events from that of opposite-charged events. The data (Drell-Yan signal plus background) are shown as circles for both dielectrons (a) and dimuons (b). Also shown, as diamonds, are the estimated contribution from heavy flavor background events as measured from $e\mu$ events.

sums of the transverse momenta of the tracks within cones in $\eta-\phi$ space [12]. The cones had a radius of 0.5 and were centered on each of the two lepton tracks. In order to be included in the sum, a track must have had a transverse momentum above 0.4 GeV/c and must not have been the lepton itself. Figures 1(a) and 1(b) show the distribution of this isolation variable for opposite- and same-charged electron and muon pairs, respectively.

Misidentification backgrounds are expected to be represented in equal amounts in events with same-charged leptons and in events with opposite-charged leptons. Indeed, we found that the isolation distributions for events failing the lepton identification cuts are charge symmetric. Therefore, we corrected for this background by subtracting the same-charge mass spectrum from the opposite-charged mass spectrum. This procedure also subtracted same-charge heavy flavor events. After subtraction, there remained the Drell-Yan signal plus the excess of the opposite-charged over same-charged heavy flavor backgrounds. To suppress the heavy flavor background we required I to be less than 1.0 GeV/c. After this cut, there were 171 e^+e^- , 13 $e^\pm e^\pm$, 81 $\mu^+\mu^-$, and 13 $\mu^\pm\mu^\pm$ events.

We estimate the background from heavy flavor events using the mass spectrum and isolation distributions observed in $e\mu$ pairs [16] which have no direct Drell-Yan contribution [17]. This background was estimated to be 19 ± 12 events in the dielectron sample and 8 ± 6 in the dimuon sample (see Fig. 2).

The efficiency of the isolation cut, ϵ_{iso} , was 0.72 ± 0.03 and 0.69 ± 0.06 in the e^+e^- and $\mu^+\mu^-$ samples, respectively, independent of pair mass. This efficiency was measured by imposing the isolation cut on leptons from Z^0 and Υ decays as well as from randomly selected directions in the isolated, opposite-charged pair events with

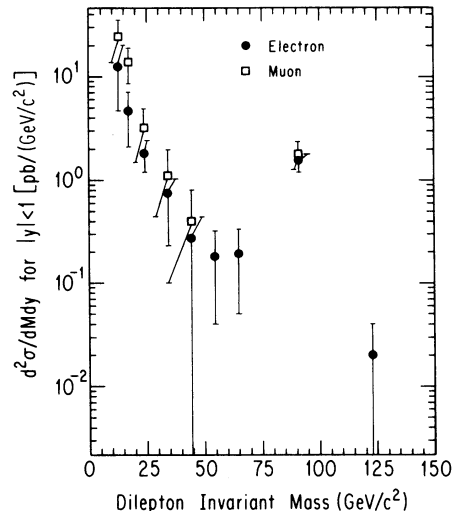


FIG. 3. The Drell-Yan differential cross section $d^2\sigma/dM dy$ as measured in the dielectron and dimuon samples plotted as a function of dilepton invariant mass.

invariant mass between 20 GeV/c² and 50 GeV/c². All methods were consistent.

Other backgrounds are small. From a study of the distributions of dimuon opening angle and track impact parameters, we estimated that 1.7 ± 0.3 cosmic-ray events survived the dimuon cuts. Using a Monte Carlo calculation we estimated 0.8 ± 0.5 dimuon events and 1.5 ± 0.1 dielectron events from the leptonic decays of τ pairs produced through the Drell-Yan process. The total number of signal and background events in each mass bin for the electron and muon samples is given in Table I.

TABLE I. Mass-dependent values used to calculate $d^2\sigma/dM dy|_{|y|<1}$ using Eq. (1). N_{OC} is the number of isolated opposite-charged events, N_{SC} is the number of isolated same-charged events, N_{bg} is the number of background events in the charge-subtracted distribution, A is the geometric and kinematic acceptance, and ϵ_{trig} is the trigger efficiency.

Mass bin (GeV)/c ²)	N_{OC}	N_{SC}	N_{bg}	A	ϵ_{trig}
			Electrons		
11–15	36	11	5.7 ± 5.4	0.18 ± 0.01	$0.47^{+0.16}_{-0.23}$
15–20	31	2	9.5 ± 7.3	0.23 ± 0.01	$0.77^{+0.03}_{-0.06}$
20–30	23	0	4.6 ± 3.6	0.25 ± 0.01	$0.90^{+0.02}_{-0.03}$
30–40	9	0	1.0 ± 0.6	0.25 ± 0.01	0.92 ± 0.05
40–50	3	0	0.21 ± 0.01	0.24 ± 0.01	0.93 ± 0.04
50–60	2	0	0.14 ± 0.01	0.23 ± 0.01	0.93 ± 0.04
60–70	2	0	0.035 ± 0.001	0.25 ± 0.01	0.93 ± 0.04
70–110	64	0	0.011 ± 0.001	0.24 ± 0.01	0.93 ± 0.04
110–150	1	0	0	0.25 ± 0.01	0.93 ± 0.04
Muons					
11–15	35	12	3.9 ± 3.9	0.078 ± 0.006	0.78 ± 0.06
15–20	18	1	2.6 ± 2.3	0.080 ± 0.006	0.81 ± 0.06
20–30	9	0	2.3 ± 1.7	0.080 ± 0.006	0.82 ± 0.07
30–40	3	0	0.7 ± 0.4	0.080 ± 0.006	0.82 ± 0.07
40–50	1	0	0.1 ± 0.1	0.080 ± 0.006	0.82 ± 0.07
50–60	0	0	0.1 ± 0.1	0.080 ± 0.006	0.82 ± 0.07
60–70	0	0	0.1 ± 0.1	0.080 ± 0.006	0.82 ± 0.07
70–110	15	0	0.1 ± 0.1	0.080 ± 0.006	0.82 ± 0.07
110–150	0	0	0	0.080 ± 0.006	0.82 ± 0.07

TABLE II. $d^2\sigma/dM dy|_{|y|<1}$ for the dielectron, dimuon, and combined samples. The first uncertainty is statistical and the second is systematic for the dielectron and dimuon samples while the combined sample has the total statistical and systematic uncertainty.

Mass bin (GeV/c ²)	Mass centroid (GeV/c ²)	Dielectron [pb/(GeV/c ²)]	Dimuon [pb/(GeV/c ²)]	Combined [21] [pb/(GeV/c ²)]
11–15	12.7	12.4±4.5 ^{+5.5} _{-7.0}	24.4±8.8±6.4	16.4±6.3
15–20	17.1	4.6±1.4 ^{+1.9} _{-2.3}	13.8±4.2±3.2	6.3±2.3
20–30	23.8	1.8±0.45 ^{+0.40} _{-0.45}	3.2±1.4±1.0	2.0±0.6
30–40	34.2	0.74±0.29±0.09	1.1±0.82±0.23	0.78±0.28
40–50	44.3	0.27±0.17±0.03	0.43±0.40±0.09	0.29±0.16
50–60	54.5	0.18±0.14±0.02	—	0.16±0.11
60–70	64.8	0.19±0.14±0.02	—	0.16±0.11
70–110	90.7	1.52±0.19±0.17	1.77±0.46±0.30	1.56±0.23
110–150	122.8	0.02±0.02±0.003	—	0.02±0.016

The acceptance due to geometric and kinematic cuts was calculated using the ISAJET Monte Carlo program [18] with the Martin-Roberts-Stirling set B [MRS(B)] parton distribution functions [19] for $|y| < 1.0$. Table I lists the combined geometric and kinematic acceptances A including a requirement that the event vertex position be within 60 cm (2σ) of the nominal interaction point along the beam axis. The main difference between the dielectron and dimuon acceptance is due to the electron detector η coverage of -1.0 to $+1.0$ while the dimuon detector η coverage is only -0.6 to $+0.6$. Table I also contains the dielectron and muon trigger efficiencies ϵ_{trig} as a function of dilepton pair invariant mass. These trigger efficiencies were measured for electrons and muons passing their respective geometric and kinematic cuts.

To calculate the differential cross section we used the formula

$$\left. \frac{d^2\sigma}{dM dy} \right|_{|y|<1} = \frac{N_{\text{OC}} - N_{\text{SC}} - N_{\text{bg}}}{\Delta M \Delta y A \epsilon_{\text{trig}} \epsilon_{\text{id}} \epsilon_{\text{isp}} \mathcal{L}}, \quad (1)$$

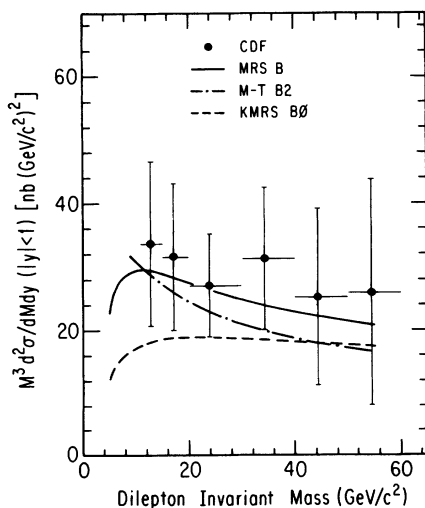


FIG. 4. The combined dielectron and dimuon Drell-Yan differential cross section $M^3 d^2\sigma/dM dy$ as a function of dilepton invariant mass, with predictions using Martin-Roberts-Stirling and Morfin-Tung distribution functions [6].

where N_{OC} is the number of isolated opposite-charged events, N_{SC} is the number of isolated same-charged events, N_{bg} is the number of background events in the charge-subtracted distribution, ΔM is the width of the mass bin, and Δy is the rapidity range of the parent boson. The cross sections are presented in Table II and are shown as a function of dilepton invariant mass in Fig. 3. The cross sections are plotted at the mass centroid of the bins. The muon cross sections are consistently higher than those of the electron. Many checks reveal no obvious cause. The muon and electron cross section calculated at the Z^0 mass agrees well with each other as well as with previous CDF measurements [5]. A statistical analysis of the overall agreement of the two sets of cross sections gives a worst case confidence level of 23%.

We obtained the total systematic uncertainty of the cross section by adding, in quadrature, the errors from the following sources. There was an uncertainty of 5% in the acceptance, A , due to varying the choice of parton-distribution functions. The systematic error in the measurement of integrated luminosity was 7% [4]. For dielectrons (dimuons), systematic errors of 4(8)% and 4(6)% were due to the uncertainties in ϵ_{iso} and ϵ_{id} , respectively. While relatively small at high mass, uncertainties due to trigger efficiency and background subtraction become dominant at low mass (see Table I).

Our combined results are shown in Fig. 4 and are consistent with the $1/M^3$ dependence that is expected from the naive Drell-Yan model. Also shown are the predictions of next-to-leading order QCD calculations [20] using several recent parton distribution functions [6]. We find better agreement with those parton distribution functions having the largest quark content in the x interval, $0.006 < x < 0.03$, covered by our data.

We thank the Fermilab staff and the technical staffs of the participating institutions for their vital contributions. We also thank James Stirling and Wu-Ki Tung for many valuable discussions. This work was supported in part by the U.S. Department of Energy and the National Science Foundation, the Italian Istituto Nazionale di Fisica Nucleare, the Ministry of Science, Culture, and Education of Japan, the Alfred P. Sloan Foundation, and the Grainger Foundation.

- [1] Y. Yamaguchi, *Nuovo Cimento* **43A**, 193 (1966); S. D. Drell and T.-M. Yan, *Phys. Rev. Lett.* **25**, 316 (1970); J. H. Christenson *et al.*, *ibid.* **25**, 1523 (1970); L. M. Lederman and B. G. Pope, *ibid.* **27**, 765 (1971).
- [2] Rapidity, y , is defined as $y = \frac{1}{2} \ln(E + p_{\parallel} / E - p_{\parallel})$ where p_{\parallel} is the longitudinal momentum along the proton beam direction and E is the energy of the lepton pair.
- [3] CDF Collaboration, F. Abe *et al.*, *Nucl. Instrum. Methods* **A271**, 387 (1988).
- [4] CDF Collaboration, F. Abe *et al.*, *Phys. Rev. D* **44**, 29 (1991).
- [5] CDF Collaboration, F. Abe *et al.*, *Phys. Rev. Lett.* **69**, 28 (1992).
- [6] Recent parton distribution functions include A. D. Martin and W. J. Stirling, *Phys. Lett. B* **248**, 443 (1990); P. N. Harriman, A. D. Martin, W. J. Stirling, and R. G. Roberts, *Phys. Rev. D* **42**, 798 (1990); J. G. Morfin and W.-K. Tung, *Z. Phys. C* **52**, 13 (1991). A review of parton distribution functions can be found in D. F. Geesaman, J. Morfin, C. Sazama, and W. K. Tung, in *Proceedings of the Workshop on Hadron Structure Functions and Parton Distributions*, Batavia, Illinois, 1990, edited by D. Geesaman *et al.* (World Scientific, Singapore, 1990).
- [7] For recent review articles, see, for example, I. R. Kenyon *Rep. Prog. Phys.* **45**, 1261 (1982); in *Proceedings of the Workshop on Drell-Yan Processes*, Batavia, Illinois, 1982 (Fermilab, Batavia, IL, 1983); C. Grosso-Pilcher and M. J. Shochet, *Annu. Rev. Nucl. Part. Sci.* **36**, 1 (1986); J. P. Rutherford, in *Proceedings of the 1985 International Symposium on Lepton and Photon Interactions at High Energies*, Kyoto, Japan, 1985, edited by M. Konuma and K. Takahashi (RIFP, Kyoto University, Kyoto, 1986), p. 661.
- [8] CDF Collaboration, F. Abe *et al.*, *Phys. Rev. Lett.* **67**, 2418 (1991); F. Abe *et al.*, *ibid.* **68**, 1463 (1992).
- [9] D. Amidei *et al.*, *Nucl. Instrum. Methods* **A269**, 51 (1988).
- [10] L. Balka *et al.*, *Nucl. Instrum. Methods* **A267**, 272 (1988).
- [11] $E_T = E \sin\theta$ and $p_T = P \sin\theta$, where θ is the polar angle measured from the proton beam direction.
- [12] η is the pseudorapidity, $-\ln[\tan(\theta/2)]$, and ϕ is the azimuthal angle in the plane perpendicular to the proton beam direction.
- [13] F. Abe *et al.*, *Phys. Rev. D* **45**, 3921 (1992).
- [14] G. Ascoli *et al.*, *Nucl. Instrum. Methods* **A268**, 33 (1988).
- [15] For muon selection details, see Victor E. Scarpine, Ph.D. thesis, University of Illinois, 1992.
- [16] CDF Collaboration, F. Abe *et al.*, *Phys. Rev. Lett.* **67**, 3351 (1991).
- [17] For details, see Kenneth Bloom, Bachelor's thesis, University of Chicago, 1992. See also Toshihiro Mimashi, Ph.D. thesis, University of Tsukuba, 1990.
- [18] F. Paige and S. Protopopescu, BNL Report No. BNL38034, 1986 (unpublished).
- [19] A. D. Martin, R. G. Roberts, and W. J. Stirling, *Phys. Rev. D* **37**, 1161 (1988).
- [20] James Stirling and Wu-Ki Tung (private communications).
- [21] We use Gaussian statistics to combine the dielectron and dimuon cross sections in the first five mass bins of Table II, and also for the bin containing the Z^0 peak. We assume that all systematic errors, except for that due to integrated luminosity, are uncorrelated. The combined cross sections for the other mass bins, where the number of events detected is small, result from the use of Poisson statistics and come from the total number of dielectron and dimuon events normalized by their respective luminosities.